10760 *Biochemistry* **1991**, *30*, 10760–10768

Billington, D., Osmundson, H., & Sherratt, H. S. A. (1978) *Biochem. Pharmacol. 27*, 2879–2890.

Bjorge, S. M., & Ballie, T. A. (1985) *Biochem. Biophys. Res. Commun. 132*, 245–252.

Cerdan, S., Kunnecke, B., Dolle, A., & Seelig, J. (1988) *J. Biol. Chem. 263*, 11664–11674.

El-Aleem, S. A., & Schulz, H. (1987) *Biochem. Pharmacol. 36*, 4307–4312.

Ellman, G. L. (1959) *Arch. Biochem. Biophys. 82*, 70–77.

Freund, K., Mizzer, J., Dick, W., & Thorpe, C. (1985) *Biochemistry 24*, 5996–6002.

Goldman, P., & Vegelos, P. R. (1961) *J. Biol. Chem. 236*, 2620–2623.

Grandell, J. K., & Tindell, G. L. (1970) *Chem. Commun.*, 1411–1412.

Hine, D. G., & Tanaka, K. (1984) *Biomed. Mass Spectrom. 11*, 332–339.

Hoppel, C. L., DiMarco, J. P., & Tandler, B. (1979) *J. Biol. Chem. 254*, 4164–4170.

Ikeda, Y., & Tanaka, K. (199) *Biochem. Biophys. Acta 1038*, 216–221.

Jager, V., & Gunther, H. J. (1977) *Tetrahedron Lett. 29*, 2543–2546.

Jin, S.-J., & Tserng, K.-Y. (1989) *J. Lipid Res. 30*, 1611–1619.

Kean, E. A. (1976) *Biochem. Biophys. Acta 422*, 8–14.

King, M. T., & Reiss, P. D. (1985) *Anal. Biochem. 146*, 173–179.

Kolvraa, S., & Gregersen, N. (1986) *Biochim. Biophys. Acta 876*, 515–525.

Melde, K., Buettner, H., Boschert, W., Wolf, H. P. O., & Ghisla, S. (1989) *Biochem. J. 259*, 921–924.

Melde, K., Jackson, S., Bartlett, K., Sherratt, H. S. A., & Ghisla, S. (1991) *Biochem. J. 274*, 395–400.

Mortensen, P. B., & Gregersen, N. (1981) *Biochim. Biophys. Acta 666*, 394–404.

Schulz, H. (1987) *Life Sci. 40*, 1443–1449.

Shaw, L., & Engel, P. C. (1985) *Biochem. J. 230*, 723–731.

Suzuki, H., Yamada, J., Watanabe, T., & Suga, T. (1989) *Biochim. Biophys. Acta 990*, 25–30.

Tanaka, K. (1972) *J. Biol. Chem. 247*, 7465–7478.

Tanaka, K., & Coates, P. M. (1990) *Fatty Acid Oxidation: Clinical, Biochemical, and Molecular Aspects*, Alan R. Liss, New York.

Tonsgard, J. H. (1989) *Lab. Invest. 60*, 568–573.

Tserng, K.-Y., Jin, S.-J., Hoppel, C. L., Kerr, D. S., & Genuth, S. M. (1989) *Metabolism 38*, 655–661.

Ullman, E. F., & Fanshawe, W. J. (1961) *J. Am. Chem. Soc. 83*, 2379–2383.

Vamecq, J., Draye, J.-P., & Brison, J. (1989) *Am. J. Physiol. 256* (*Gastrointest. Liver Physiol. 19*), G680–G688.

Viancy-Liaud, C., Divry, P., Gregersen, N., & Mathieu, M. (1987) *J. Inherited Metab. Dis. 10* (Suppl. 1), 159–198.

Wenz, A., Thorpe, C., & Ghisla, S. (1981) *J. Biol. Chem. 256*, 9809–9812.

Wenz, A., Ghisla, S., & Thorpe, C. (1985) *Eur. J. Biochem. 147*, 533–560.

Zhou, J.-Z., & Thorpe, C. (1989) *Arch. Biochem. Biophys. 271*, 261–269.

Multibilayer Structure of Dimyristoylphosphatidylcholine Dihydrate As Determined by Energy Minimization†

Garret Vanderkooi

Department of Chemistry, Northern Illinois University, DeKalb, Illinois 60115

Received July 2, 1991; Revised Manuscript Received August 15, 1991

ABSTRACT: Complete energy minimization was carried out on the multibilayer crystal structure of 1,2-dimyristoyl-*sn*-glycero-3-phosphocholine dihydrate ($\mathrm{DMPC{\cdot}2H_2O}$), starting from the X-ray structure determination reported by Pearson and Pascher (1979) *Nature 281*, 499–501. The asymmetric unit contains two nonidentical DMPC molecules and four water molecules. Minimization removed the acyl chain disorder present in the X-ray structure and caused the carbon planes of the acyl chains to become mutually parallel. Two energy-minimized structures (structures I and II) were found which mainly differed in the hydrogen-bonding arrangement of the waters of hydration. In structure I as in the X-ray structure, one of the water molecules forms a hydrogen-bonded bridge between successive bilayers; but in structure II, all hydrogen bonds are satisfied on the same bilayer. Structure II corresponds to the global energy minimum and is also a suitable structure for single bilayers. The lattice constants and cell volume of the minimized structures are close to the experimental values. The electrostatic force between DMPC bilayers is attractive. The mean hydration energy of the water is −14.2 kcal/mol, which is 2.5 kcal/mol lower than the binding energy of ice.

Energy minimization has been carried out on multibilayers of 1,2-dimyristoyl-*sn*-glycero-3-phosphocholine dihydrate (dimyristoylphosphatidylcholine dihydrate, $\mathrm{DMPC{\cdot}2H_2O}$),[1] using the X-ray crystal structure reported by Pearson and Pascher (1979) as the starting point.

Structural studies of phosphatidylcholines have been made by X-ray analysis, neutron diffraction, and NMR. The most

---

†Supported in part by Grant BRSG S07 RR07176 from the Biomedical Support Grant Program, Division of Research Resources, National Institutes of Health.

[1] Abbreviations: DMPC, 1,2-dimyristoyl-*sn*-glycero-3-phosphocholine; DLPE·HAc, 1,2-dilauroyl-DL-phosphatidylethanolamine–acetic acid; DLPEM$_2$, 2,3-dilauroyl-DL-glycero-1-phospho-*N*,*N*-dimethylethanolamine; DLG, 2,3-dilauroyl-D-glycerol; lysoPE, 3-palmitoyl-DL-glycero-1-phosphoethanolamine; DMPC1 and DMPC2, DMPC molecules 1 and 2 in the $\mathrm{DMPC{\cdot}2H_2O}$ crystal structure; W1, W2, W3, and W4, water molecules in the $\mathrm{DMPC{\cdot}2H_2O}$ crystal structure.

0006-2960/91/0430-10760$02.50/0

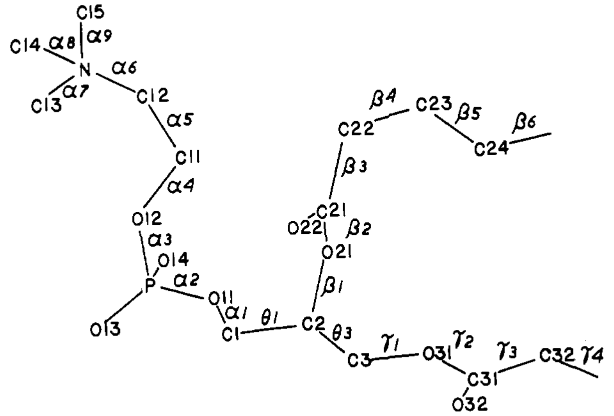

FIGURE 1: Bond and atom labeling scheme for DMPC (Sundaralingam, 1972).

definitive structural study to date is the single-crystal three-dimensional X-ray structural analysis of Pearson and Pascher (1979). The crystals employed in that work consisted of stacked multibilayers in the gel state, with two DMPC molecules and four water molecules in the asymmetric unit. The DMPC molecules had different conformations and were offset relative to each other by 2.5 Å normal to the bilayer plane. Neutron diffraction measurements have also been carried out on oriented multibilayers of specifically deuterated dipalmitoylphosphatidylcholines at different hydration levels and at temperatures both below and above the thermal phase transition (Büldt et al., 1979; Zaccai et al., 1979). These studies showed that the phosphocholine group was approximately parallel to the bilayer plane under all conditions employed, in agreement with the X-ray results on the dihydrate (Pearson & Pascher, 1979).

Information on the rotamer populations of the glycerol group in phosphatides has been obtained by NMR using short-chain micelle-forming phospholipids. Hauser et al. (1988) measured the spin–spin coupling constants of the glycerol region in micelles of 1,2-dihexanoyl-*sn*-glycero-3-phosphocholine and 1,2-dihexanoyl-*sn*-glycero-3-phosphoethanolamine. They found two rotameric states (A and B) for the C2–C3 glycerol bond. (The atom numbering system of Sundaralingam (1972) is employed; see Figure 1.) The dihedral angle θ_3, defined by atoms C1–C2–C3–O31, is antiperiplanar (≈180°) in rotamer A and is +synclinal (≈60°) in rotamer B. Rotamers A and B were estimated to be present in about a 2:1 ratio. Similar rotamer populations were found by Basti and LaPlanche (1990) for 1,2-dioctanoyl-*sn*-glycero-3-phosphocholine in chloroform–methanol solution. Comparison with the crystal literature shows that rotamer A is found in the structure of DMPC·$2H_2O$ (Pearson & Pascher, 1979) and in 2,3-dilauroyl-DL-glycero-1-phosphoethanolamine–acetic acid (DLPE·HAc) (Hitchcock et al., 1974; Elder et al., 1977) but that rotamer B gives the layer perpendicular head-group orientation which is present in the crystal structure of 2,3-dilauroyl-DL-glycero-1-phospho-*N*,*N*-dimethylethanolamine ($DLPEM_2$) (Pascher & Sundell, 1986). The NMR results indicate that the dynamic structures of phosphatide polar groups may be more varied than those which are found in the crystals.

The earliest phosphatide conformational calculations on isolated molecules were reported by McAlister et al. (1973) and Vanderkooi (1973). These groups each showed that only a few conformations of the glycerol group in phosphatides are possible on account of steric hindrance. Isolated molecule calculations were also carried out by Pullman and Saran (1975) using the PCILO method. Their work was done after the publication of the DLPE·HAc crystal structure by Hitchcock et al. (1974). According to their calculations, the intramolecular energy of DLPE in the conformation found in the crystal was 2 kcal/mol above the global minimum. They concluded from this that intermolecular interactions must be important in determining the DLPE conformation in the bilayer. Since then, a few groups have carried out limited studies on the role of intermolecular interactions in bilayer structure. Frischleder (1978, 1980) and Frischleder and Lochman (1979) investigated the effects of intermolecular interactions on the head-group conformations of phosphatidylethanolamine and phosphatidylcholine using a two-dimensional crystal lattice consisting only of a monolayer of polar groups, while Brasseur et al. (1981) and Kreissler et al. (1983) each carried out energy calculations on isolated clusters of seven molecules in a monolayer arrangement without using symmetry. The presence of potentially large uncompensated edge effects around the periphery of the clusters was ignored in the latter studies. This problem can be avoided by using crystal symmetry to generate an entire two- or three-dimensional array.

The energy minimization approach to molecular structure determination is mainly useful for studying monomeric or multimeric systems in which there are a limited number of stable structures defined by relatively deep and narrow energy wells. Crystal structures in general satisfy this requirement, but fluid systems do not. In the case of lipid bilayers, the molecular motions in the gel state are sufficiently restricted so that this state can be studied by energy minimization, but these methods are not appropriate for general use with the liquid-crystalline state due to its fluidity. Molecular dynamics methodology is being developed in other laboratories for studying the structural characteristics of micelles (Wendoloski et al., 1989) and liquid-crystalline bilayers (DeLoof et al., 1991; Pastor et al., 1991).

The approach taken in the present series of calculations is to use the known crystal structures of bilayer lipids as starting points for energy minimization calculations (Vanderkooi, 1990a,b). This approach assures that a close link is maintained between theory and experiment. Calculations have been made on good quality crystal structures of two lipids, viz., 2,3-dilauroyl-D-glycerol (DLG) (Pascher & Sundell, 1981a), and 3-palmitoyl-DL-glycero-1-phosphoethanolamine (lysoPE), (Pascher & Sundell, 1981b). Close agreement was found between the experimental and the energy-minimized structures of both of these crystals (Vanderkooi, 1990b), which provides a basis for confidence in using the same methods to carry out energy refinement calculations on crystal data of lower quality. Energy refinement calculations have been made on DLPE·HAc (Vanderkooi, 1990a,b) and DMPC·$2H_2O$ (present work). In addition to providing structural information, the energy calculations give a quantitative insight into the relative magnitudes of the various energy components involved in holding bilayers and multibilayers together and also offer the possibility of studying other structures and conformations which may not be accessible to investigation by experimental means.

MATERIALS AND METHODS

DMPC X-ray Structure. The crystal structure of DMPC·$2H_2O$ was reported by Pearson and Pascher (1979), with further details having been given by Hauser et al. (1981). This lipid forms monoclinic crystals in the $P2_1$ space group with unit cell dimensions of $a = 8.72$ Å, $b = 8.92$ Å, $c = 55.4$ Å, and $\beta = 97.4°$. There are two DMPC molecules and four water molecules in the crystallographic asymmetric unit and two asymmetric units in the unit cell related by a 2-fold screw axis. The DMPC molecules are in a typical lamellar multibilayer arrangement, and the water molecules are associated with the polar head groups.

Idealized Structure. The bond lengths and angles calculated from the X-ray coordinates for DMPC showed appreciable variations from expected values. Coordinates were therefore generated using standard bond lengths and angles. Values given by Weiner et al. (1984) were used for most bonds. All C–H bond lengths were set at 1.09 Å. Standard geometry for the carboxylic ester group was determined from a survey of the crystal literature of compounds which have ester groups in similar environments to those found in phosphatides. This idealized DMPC structure was fitted to the X-ray coordinates of each of the two DMPC molecules in the crystal by minimizing the sum of the squares of the distances between the respective pairs of X-ray atoms and ideal atoms as a function of bond rotations, rigid body translations, and rigid body rotations of the ideal structure. The mean deviation of the fitted ideal coordinates from the X-ray coordinates was 0.14 Å, and the maximum deviation was 0.37 Å. The idealized structure obtained in this manner will be referred to as the initial structure, which was used as the starting point for subsequent energy minimizations.

Energy Functions and Parameters. The empirical crystal energy was computed as the sum of intramolecular and intermolecular interactions and included nonbonded, electrostatic, hydrogen-bonded, and torsional energy terms. The intermolecular energy included pairwise interatomic interactions among the six molecules in the asymmetric unit and between the reference asymmetric unit and the surrounding environment generated by symmetry, out to a nominal cutoff distance of 12 Å. The energy functions of Momany et al. (1974) were employed together with the energy parameters of Momany et al. (1974), Sippl et al. (1984), and Vanderkooi (1983). Hydrogen-bonding parameters for interactions involving water were reevaluated, and the results are given below. Details of the computational methods were given by Vanderkooi (1990a).

Energy Minimization. The total crystal energy was minimized as a function of all bond rotations, molecular rotations and translations, and the lattice constants, using the methods previously described (Vanderkooi, 1990a). The DUMING derivative-based unconstrained minimization program was used (IMSL Math Library, version 1.0, 1987). First derivatives of the energy were computed analytically with respect to all variables, and all variables were permitted to change simultaneously during the course of minimization. There were 121 minimization variables for the DMPC·H_2O crystal. All calculations were carried out on the Amdahl 5890 mainframe computer at Northern Illinois University.

Hydrogen-Bonding Parameters for Water. In the energy parameter refinement studies of Vanderkooi (1983), the hydrogen-bond parameters for water–water interactions were equated to those given by Nêmethy and Scheraga (1977) for alcohol interactions. Energy minimization of the crystal structure of ordinary ice showed, however, that these parameters gave a shrinkage of the ice lattice. The 10–12 hydrogen-bond function was therefore reparameterized for water, with water and alcohol hydroxyl hydrogens being treated as different atom types.

The crystal structure of ice at 0 °C was generated using the lattice constants given by Wyckoff (1963). An asymmetric unit consisting of four water molecules was employed. A bond length of 0.9572 Å and an angle of 104.52° were used for the water molecule (Benedict et al., 1956). Partial charges of −0.66 and 0.33 electron units were assigned to the O and H atoms, respectively (Weiner et al., 1984); these charges reproduce the experimental dipole moment of 1.84 D. A dielectric constant of 2.0 was used for calculating the electrostatic energy in order to maintain computational consistency with previous methodology. The experimental lattice constants and the energy of sublimation of ice at 0 °C (11.66 kcal/mol; Rossini et al., 1952) were used to empirically adjust the water hydrogen-bond parameters. The crystal energy and the energy-minimized lattice constants for ice obtained with the new parameters closely reproduce the experimental values. Table I gives the parameters so obtained.

Table I: Hydrogen-Bonding Parameters for Water[a]

atom pair[b]	r_0 (Å)	ϵ (kcal/mol)
H_{12}–O_{18}	1.80	3.72
H_{12}–O_{23}	1.75	3.72
H_{12}–O_{24}	1.80	3.72
H_{22}–O_{18}	1.80	3.72

[a] The parameters for other types of hydrogen bonds are as given by Vanderkooi (1983) and Sippl et al. (1984). [b] Atom type designations: H_{12}, water hydrogen; H_{22}, phosphoric acid hydrogen; O_{18}, water, alcohol, carboxyl, and carboxylic ester oxygen; O_{23}, phosphoryl and phosphate oxygen; O_{24}, phosphate ester and phosphoric acid oxygen.

A revised set of hydrogen-bond parameters was also derived for interactions between water and the phosphate group. The alcohol–phosphate hydrogen-bond parameters originally obtained were retained (Vanderkooi, 1983), but new values were determined for water–phosphate interactions. The depth of the potential function for all hydrogen bonds in which water is the hydrogen donor was set at the same value as for water–water interactions (3.72 kcal/mol), and the positions of the minima for the different bond types were determined from energy minimizations on the several organic phosphate crystal structures containing water which were used in the earlier work. This resulted in an appreciably improved fit between the experimental and computed lattice constants for the crystals. The final parameters are included in Table I.

RESULTS

Energy Minimization. The energy of the DMPC·$2H_2O$ crystal structure was minimized with respect to all bond rotations, rigid body motions, and the lattice constants, starting from the initial structure which was obtained from the X-ray structure as described under Materials and Methods. Several geometrical arrangements for the water molecules were tried in addition to the one indicated by the X-ray analysis. Complete energy minimizations were carried out for four different water hydrogen-bonding patterns, with each of them yielding a different minimized structure. In each case, changes occurred in the conformations of the DMPC molecules as required to optimize the interactions with the water molecules. Detailed results are given for two of the energy-minimized structures obtained in this manner; these will be referred to as structures I and II. The hydrogen bonding in structure I is similar to that in the X-ray structure, with one of the water molecules forming a hydrogen-bonded bridge between adjacent bilayers. In structure II all of the water hydrogen bonds are between groups in the same bilayer, with no interbilayer bridges being present. Both arrangements give stable multibilayer structures, but structure II is also nearly equivalent to the energy-minimized single bilayer structure. The total energy of structure II is lower than that of structure I by 2.54 kcal/mol and corresponds to the global minimum.

Lattice Spacings and Bilayer Parameters. Table II gives the unit cell dimensions and various other geometrical data

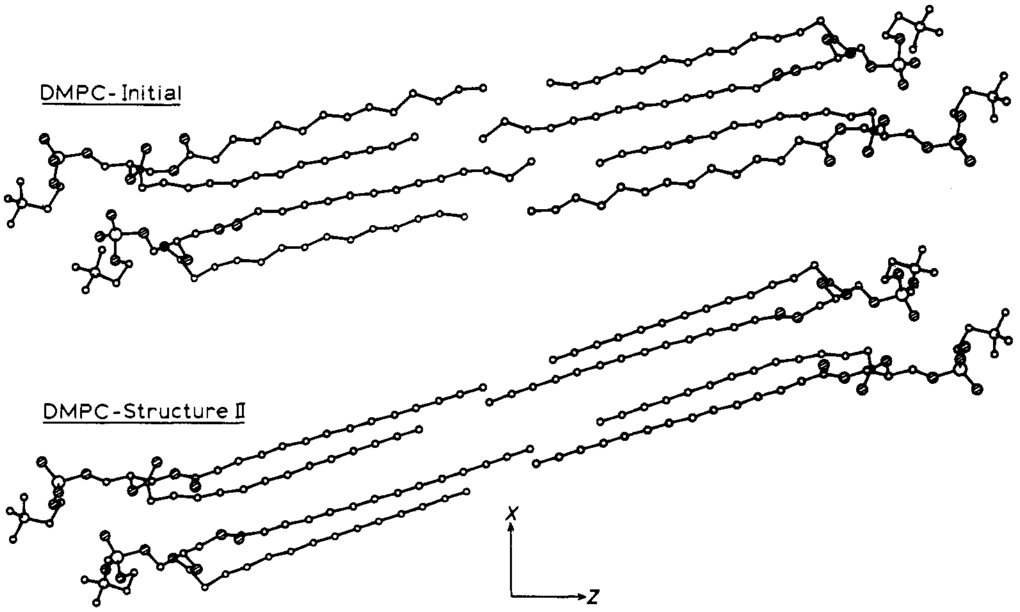

FIGURE 2: Comparison of the molecular conformations and bilayer packing of the initial (upper) and energy-minimized conformations (lower, structure II). The water molecules and hydrogen atoms have been omitted for clarity, and the oxygen atoms are hatched. The projection is down the *b* crystal axis. The orientation of the Cartesian coordinate system is indicated; *x* is parallel to the *a* crystal axis and lies in the bilayer plane, and *z* is normal to the bilayer plane. The lengths of the coordinate vectors correspond to 4 Å.

for the minimized structures, as well as the corresponding values for the initial (X-ray) structure. The lattice constants and unit cell volume changed by only a small amount as a result of energy minimization. The maximum change in cell dimensions for structure II was 0.15 Å (1.7%), and the minimized cell volume was within experimental error of the X-ray value. The surface area per molecule and the bilayer repeat distance also changed by less than 1%. A numerically larger change occurred in the β lattice angle, which decreased from 97.4° to 91.1° (structure I) or 93.1° (structure II). The results show that the minimized structures are compatible with the experimental lattice; the only constraint imposed on the system in the course of the minimization was that the space group must remain unchanged.

The thickness of the nonpolar acyl chain region was unchanged as a result of minimization, but the interbilayer spacing decreased by 0.2 Å in structure I and increased by 0.4 Å in structure II (Table II). The shorter interbilayer spacing in structure I than in structure II is the result of the presence of the interbilayer water bridge which is present only in structure I. The nonpolar region thickness and the interbilayer spacing are calculated as the distances between the median planes defined by the C2 glycerol atoms of DMPC1 and DMPC2.

Molecular Conformation: Acyl Chains. The terminal portions of the acyl chains showed considerable disorder in the X-ray structure as evidenced by variable bond lengths, bond angles, and bond rotations. The bond rotations in the initial structure differed by up to 40° from planarity in the terminal parts of the chains, but minimization caused all of these angles to become close to 180°. The mean carbon atom planes of the β and γ chains in both of the DMPC molecules were set at angles of about 45° to each other in the crystal structure, but in the minimized structures these planes rotated so that all four carbon chains in the asymmetric unit were within 10° of being mutually parallel. The chain reorientations involved a 65° rotation about $\gamma 1$ in DMPC2, from 116° to 181°, and smaller distributed changes (by up to 40°) in $\beta 5$, $\beta 6$, and $\gamma 1$ to $\gamma 4$ of DMPC1. The effects of these changes can be visualized in Figure 2 in which structure II is compared with the initial structure. (The acyl chain conformation of structure I is similar to that of II.) The molecules are projected onto the *ac* lattice plane in Figure 2, which is also the *xz* plane in Cartesian coordinates. The acyl chains for the minimized structure appear as nearly straight lines since the carbon planes are perpendicular to the *ac* plane, but this is clearly not the case for the X-ray structure. The dihedral angles are given in Table III for the initial and energy-minimized DMPC conformations.

The straightening of the acyl chains which occurred upon minimization inevitably also caused the chains to become somewhat longer and to have a smaller mean cross-sectional chain area than in the initial structure. This conformational change provides the basis for understanding the changes in tilt angle and in the β lattice angle which also occurred (see

Table II: Geometrical Parameters for the Energy-Minimized DMPC·$2H_2O$ Crystal Structures

parameter	structure		
	initial	I	II
lattice constants (Å, deg)			
a	8.72	8.644	8.573
b	8.92	8.982	9.000
c	55.35	54.556	55.331
α	90.0	90.0	90.0
β	97.4	91.08	93.13
γ	90.0	90.0	90.0
unit cell vol (Å^3)	4269	4235	4263
surface area per mol·(Å^2)	38.89	38.82	38.58
bilayer repeat dist (Å)	54.89	54.55	55.25
nonpolar region thickness (Å)[a]	38.6	38.5	38.6
polar region thickness (Å)[a]	16.3	16.1	16.7
molecular offset (Å)[b]	2.50	2.76	2.86
acyl chain tilt (deg)[c]	12.4	18.3	17.9
P–N vector angle (deg)[d]			
DMPC1	15.9	9.8	9.4
DMPC2	27.6	26.2	24.7

[a] The boundary between the polar and nonpolar regions is defined by the midplane between the C2 atoms in the glycerol groups of DMPC1 and DMPC2. [b] The molecular offset is the distance between the planes defined by the C2 atoms of DMPC1 and DMPC2. [c] The tilt angle is measured relative to the bilayer normal. [d] The P–N vector angle is measured with respect to the bilayer plane.

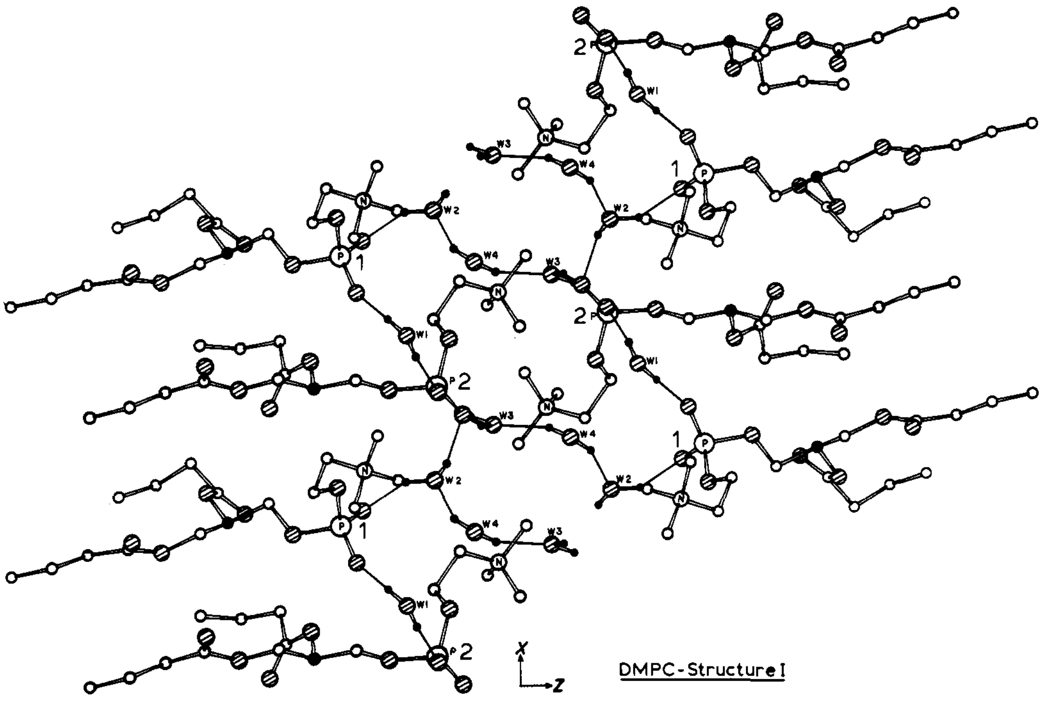

FIGURE 3: Detail showing the hydration arrangement in structure I. The projection is the same as in Figure 2; the lengths of the coordinate vectors correspond to 1 Å. The hydrogen atoms of the water molecules are shown as filled circles, and the hydrogen bonds are indicated as solid lines. The C2 glycerol atoms are also filled, and the oxygens are hatched. The hydrogen bonds are shown in projection and include some bonds which originate or terminate in the unit cells above or below the plane of the paper.

Table II). The tilt angle increased from 12.4° to about 18°, as required to maintain the same aliphatic chain area as projected on the bilayer plane. This in turn caused a change in the β angle; β controls the positioning of successive monolayers in the a lattice direction. The β angle changed as needed to maintain the same register of the terminal CH_3 groups at the bilayer midplanes.

Polar Group Conformation. The phosphocholine group has very little conformational freedom of motion beyond the $\alpha1$ bond. The positively charged quaternary ammonium group bends back to approach the negative phosphate group on either the right or the left side, in two locally equivalent mirror image conformations. One of these occurs in DMPC1, and the other in DMPC2. The entire phosphocholine group can reorient as a unit by rotations about the $\theta1$ and $\alpha1$ bonds (Vanderkooi, 1973); $\theta1$ is +synclinal in DMPC1 and is antiperiplanar in DMPC2, which accounts for the different dispositions of the two polar groups. The P^-–N^+ vector makes an angle of 25°–27° with the bilayer plane in DMPC2, but only 9°–16° in DMPC1 (Table II). The two DMPC molecules are also offset in the direction of the bilayer normal by 2.5 Å in the X-ray structure and by 2.8 Å in the minimized structures, with DMPC2 extending the greater distance into the interbilayer space.

Hydration. The hydrogen-bonded arrangement of the water molecules in structure I is similar to that found in the X-ray structure and includes one water molecule which acts as a hydrogen-bonded bridge linking successive bilayers together. In structure II, on the other hand, all hydrogen-bonded interactions are between molecules which are part of the same bilayer. Table IV lists the hydrogen bonds in both structures. Structure II has a total of eight hydrogen bonds, but structure I has only seven; one of the hydrogen atoms on W3 in structure I does not participate in a bond.

In both of the minimized structures, water molecules W1 and W2 form hydrogen-bonded links between phosphate oxygens of adjacent DMPC molecules in the same bilayer, and H1 of W3 is bonded to the phosphate group of DMPC2. H2 and W3 is not involved in hydrogen bonding in structure I (nor in the X-ray structure) but is bonded to W2 in structure II. H1 of W4 is bonded to the oxygen of W2 in both structures; but H2 of W4 makes an interbilayer bridge in structure I, being bonded to a symmetry-related W3 molecule of the next bilayer, whereas in structure II this hydrogen is bonded to a phosphate oxygen in the same bilayer. The hydrogen-bonded networks are illustrated in Figures 3 and 4.

Table III: Dihedral Angles About Bonds in the Polar Parts of the Initial Structure and the Energy-Minimized DMPC Structures[a]

dihedral angle (deg)	DMPC1			DMPC2		
	initial[b]	I	II	initial[b]	I	II
$\theta1$	58.8	67.8	69.8	163.6	178.3	173.0
$\theta3$	168.3	181.2	178.7	177.0	184.2	184.0
$\alpha1$	160.5	169.4	168.6	163.5	183.2	168.8
$\alpha2$	59.6	63.6	69.3	286.8	270.7	259.7
$\alpha3$	65.1	59.8	57.7	303.7	321.8	316.5
$\alpha4$	151.7	161.1	158.2	199.0	198.1	191.6
$\alpha5$	283.3	276.4	277.8	79.0	83.9	82.1
$\alpha6$	69.0	56.0	53.7	291.3	310.1	306.8
$\beta1$	92.5	85.1	82.1	135.6	155.1	157.7
$\beta2$	174.8	175.9	181.1	174.6	172.4	171.8
$\beta3$	258.4	260.2	263.5	210.8	199.7	198.8
$\beta4$	77.0	77.6	77.1	70.7	64.5	64.3
$\beta5$	149.3	173.0	172.9	179.2	183.7	180.4
$\beta6$	160.7	183.5	183.3	168.1	168.6	168.3
$\gamma1$	180.5	204.1	204.2	116.4	184.1	180.7
$\gamma2$	196.5	158.9	156.8	165.9	178.2	178.2
$\gamma3$	199.1	158.3	160.6	169.1	146.3	148.5
$\gamma4$	168.4	183.8	182.8	192.7	178.6	176.6
$\gamma5$	171.6	180.2	180.1	196.4	181.3	181.8
$\gamma6$	178.6	182.3	181.8	168.2	179.1	177.7

[a] The angles beyond $\beta6$ and $\gamma6$ are close to 180° in the minimized structures. [b] The angles given are for the initial structure and differ somewhat from the dihedral angles given by Hauser et al. (1981) for the X-ray structure.

All of the water–phosphate bonds in structures I and II involved the nonesterified phosphate oxygens, but in another low-energy structure obtained by minimization (not reported) a hydrogen bond was present between water and one of the

Table IV: Hydrogen-Bond Distances in Energy-Minimized DMPC·$2H_2O$ Crystals

			distances (Å)			
			structure I		structure II	
donor water	atom	acceptor[a] (mol., atom, sym. op.)	O–O	H–O	O–O	H–O
W1	H1	DMPC2, O13, $y = -1$	2.707	1.753	2.681	1.748
	H2	DMPC1, O13	2.705	1.754	2.649	1.748
W2	H1	DMPC1, O14, $y = 1$	2.608	1.736	2.656	1.720
	H2	DMPC2, O14, $x = 1$	2.622	1.760	2.595	1.770
W3	H1	DMPC2, O14, $x = 1$	2.675	1.737	2.628	1.750
	H2	W2	(not bonded)		2.628	1.835
W4	H1	W2	2.709	1.803	2.739	1.827
	H2	W3 $(1 - x, y + 0.5, -z)$[b]	2.676	1.823	(not bonded)	
	H2	DMPC2, O13	(not bonded)		2.697	1.763

[a] The symmetry operations are given in terms of the unit cell coordinates for generating the acceptor molecule from the reference asymmetric unit; the acceptor is part of the reference asymmetric unit if the symmetry operation is not given. [b] Interbilayer hydrogen bond.

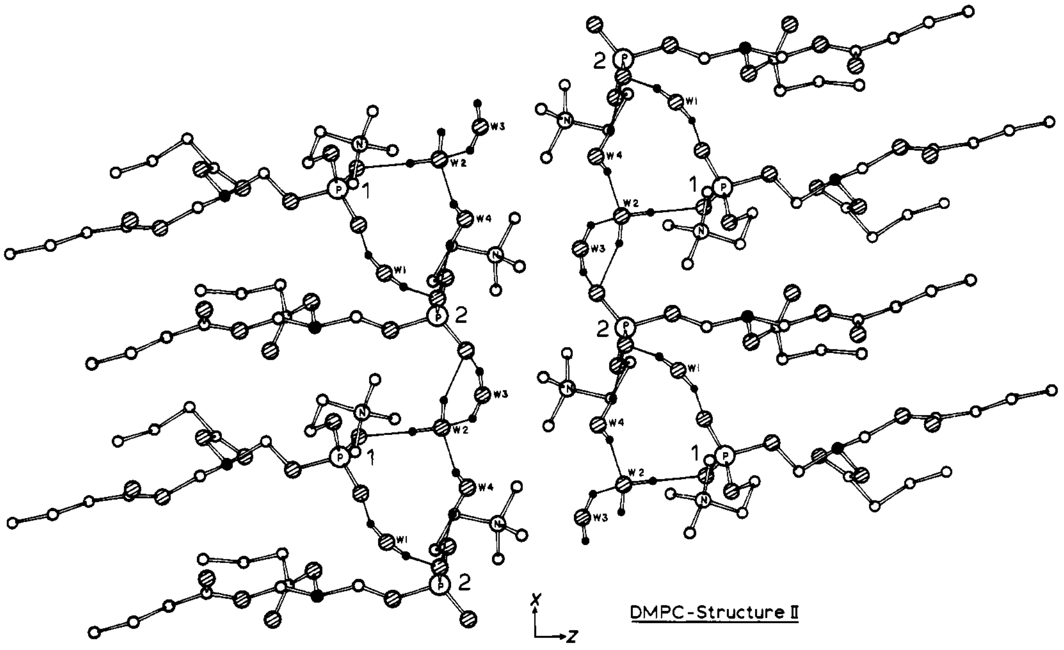

FIGURE 4: Hydration arrangement in structure II. See the legend to Figure 3.

esterified phosphate oxygens (O12), showing that this kind of hydrogen bond is also possible and should be considered in structural studies.

Bilayer Energetics. The intermolecular and intramolecular energies are given in Table V for each molecule in the two energy-minimized structures. No energies are reported for the initial structure since these were artificially high due to trivial atomic overlaps. The intramolecular energies of the two DMPC molecules in the asymmetric unit differ by a small amount, with the energy of DMPC1 being lower than DMPC2 by 1.0–1.7 kcal/mol. There is little difference in the total intramolecular energy between structures I and II.

The intermolecular energies for the individual molecules given in Table V were calculated by assigning half of the energy of each pairwise interaction to each of the molecules involved. The intermolecular energy of DMPC2 is lower than that of DMPC1 by 5.2 ± 0.1 kcal/mol in both structures. Greater variation is seen in the water molecule energies. The largest difference is for W2 (−10.25 kcal/mol in structure I, vs −13.08 kcal/mol in structure II); this is a result of the fact that W2 is involved in four hydrogen bonds in structure II but only three in structure I (see Table IV). The total water molecule energy is also lower in structure II than in structure I (−36.79 kcal/mol in structure I vs −39.42 kcal/mol in structure II). The difference of 2.63 kcal/mol between the water molecule energies mainly accounts for the difference in total energy (2.54 kcal/mol) between the two structures. The energy change which would occur upon removal of the water molecules from the crystal structure is greater than the sum of the individual water molecule energies, however, since their removal would also cause changes in the intermolecular energy of the DMPC molecules.

Table V: Individual Molecule Energies in DMPC·$2H_2O$ Crystals

energy term (kcal/mol)	structure I	structure II
intramolecular		
DMPC1	−33.54	−33.93
DMPC2	−32.53	−32.23
total	−66.07	−66.16
intermolecular		
DMPC1	−76.04	−76.04
DMPC2	−81.33	−81.15
W1	−10.10	−9.49
W2	−10.25	−13.08
W3	−8.06	−7.73
W4	−8.38	−9.12
total	−194.16	−196.61
intra- + intermolecular	−260.23	−262.77

From the data in Table V, one might conclude that the two minimized structures are essentially identical except for the water molecules, since the energies of the DMPC molecules are nearly the same in both cases. A further breakdown and analysis of the energy terms shows this is not so; the near equivalence of the total DMPC energies is a result of com-

Table VI: Components of the Intermolecular Energy of $DMPC{\cdot}2H_2O$ Crystals

energy term (kcal/mol)[a]	structure I[b]		structure II[b]	
	$+H_2O$	$-H_2O$	$+H_2O$	$-H_2O$
lateral				
nonbonded	−108.64	−101.32	−106.86	−101.95
electrostatic	−33.34	−9.05	−40.79	−8.64
hydrogen bonded	−23.77	0.0	−32.18	0.0
total	−165.75	−110.37	−179.83	−110.59
intrabilayer				
nonbonded	−6.01	−6.01	−6.00	−6.00
interbilayer				
nonbonded	−9.56	−7.36	−6.98	−5.13
electrostatic	−8.92	−7.51	−3.78	−4.49
hydrogen bonded	−3.93	0.0	−0.02	0.0
total	−22.41	−14.87	−10.78	−9.62

[a] Lateral interactions are between molecules in the same monolayer. The intrabilayer interactions are between the two monolayers of the same bilayer. The interbilayer interactions are between successive bilayers in the multibilayer crystal. The energy is expressed per mole of asymmetric unit, with the asymmetric unit containing two molecules of DMPC and four molecules of water in the hydrated case, or only two molecules of DMPC in the anhydrous case. [b] The anhydrous crystals ($-H_2O$) differ from the hydrated crystals ($+H_2O$) only in that the four water molecules were removed for the energy calculation; the structures are otherwise identical.

pensation between quite different values for the various energy terms (see Table VI).

Lateral, Intrabilayer, and Interbilayer Energies. The components of the intermolecular energy are given in Table VI for interactions between molecules in the same monolayer (lateral interactions), between monolayers in the same bilayer (intrabilayer interactions), and between bilayers (interbilayer interactions). Also shown are the corresponding energy values calculated with the omission of the water molecules, but without reminimizing or otherwise changing the structures.

The lateral energy is lower in structure II than in structure I, but the interbilayer energy is lower in structure I than in structure II. In the absence of water, the lateral energies are equivalent in the two structures, but the interbilayer energy is still lower in structure I than in structure II on account of more favorable nonbonded and electrostatic interactions. The nonbonded energy makes the largest contribution to the lateral energy as a result of extensive interactions between the parallel acyl chains, and the intrabilayer energy is entirely due to nonbonded interactions.

Electrostatic Force between Bilayers. It can be seen from Table VI that the electrostatic energy between bilayers is negative at the energy minimum and that this is true both with and without water present. The sign and magnitude of the electrostatic energy do not indicate whether the electrostatic force is attractive or repulsive, however. This can be determined from the dependence of the energy on distance, since the slope of a plot of energy versus distance gives the negative of the force. The net charge on each bilayer surface is zero, which means that the electrostatic force is due to dipolar interactions, and this may be positive or negative depending upon the detailed geometry. The interbilayer energy and its electrostatic component are plotted in Figure 5 as a function of the interbilayer distance for structure II. (The distance dependence of the energy of structure I was qualitatively similar to that shown here, except that the depth at the minimum was lower due to the overall stronger interbilayer interactions.) The electrostatic energy is seen to change monotonically and with a positive slope; this shows that the electrostatic force between the DMPC bilayers is attractive. The corresponding interbilayer energy functions are also shown in Figure 5 for the anhydrous crystal. The removal of water caused the position of the energy minimum to shift to a somewhat shorter location but did not change the attractive nature of the interbilayer electrostatic force.

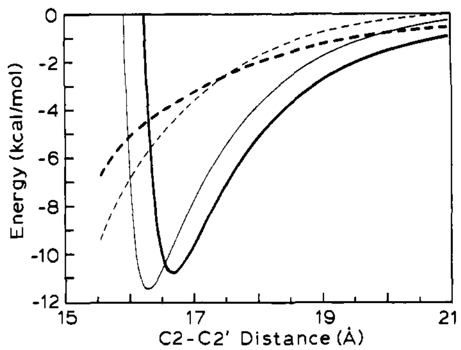

FIGURE 5: Dependence of the interbilayer energy of structure II on the interbilayer separation distance. The separation distance is measured from the median plane of the C2 atoms of DMPC1 and DMPC2 in one bilayer to the corresponding plane in the other bilayer. The interbilayer energy for the dihydrate is given by the heavy solid line, and the energy for the anhydrous structure is given by the fine solid line. The dashed heavy and fine lines give the electrostatic component of the total energy for the hydrated and anhydrous bilayers, respectively.

The energy curves in Figure 5 are quantitatively valid only at distances close to the energy minimum, since in a real system the intervening space at larger separations would necessarily be filled with additional water molecules. The presence of additional water in the interbilayer space would not be expected to change the qualitative results, however, but would be expected to cause the energy to approach zero more rapidly than is shown here.

The electrostatic energy between bilayers must necessarily be a function of the relative lateral positions of the two bilayers. In the case of the DMPC crystal, a 2-fold screw axis parallel to the bilayer plane relates the apposed bilayers; this gives a half-cell translation parallel to the *b* lattice vector and causes the two bilayers to be staggered by that amount. This offset permits the more extended polar groups of DMPC2 to fit into the surface depressions of the DMPC1 molecules in the other bilayer and also, as is evident from Figure 5, results in favorable electrostatic interactions. If, on the other hand, a mirror plane related the two bilayers, the electrostatic force would be repulsive since like charges would be directly opposite each other across the mirror plane. (A mirror plane would not actually be possible for DMPC, on account of its chiral center.) The point of this argument is to show that when two bilayers approach each other, their lateral alignment will be influenced by their general surface contours and also by their electrostatic fields, and a lateral shift by only a few angstroms may make the difference between the electrostatic force between bilayers being attractive or repulsive.

DISCUSSION

The two low-energy structures found by energy minimization of the $DMPC{\cdot}2H_2O$ crystal differ mainly in the hydrogen-bonding arrangement of the hydrated water molecules. This arrangement is the same in structure I as in the X-ray structure, but structure II, which has a different arrangement, has the lowest total energy. Both structures I and II form stable multibilayer crystals, although the interbilayer energy is lower in structure I than in structure II as a result of the interbilayer hydrogen-bonded bridge in structure I.

Energy minimization of an isolated single bilayer of $DMPC{\cdot}2H_2O$ yielded a structure which was virtually identical to structure II, showing that structure II is also an acceptable structure for single bilayers. This is not the case for structure

I, however, since the interbilayer water bridge is broken if the bilayers are separated.

Conformational Changes. The lattice dimensions and bilayer spacings of the energy-minimized crystal structures were nearly identical to the experimental values, but the conformations of the aliphatic chains showed appreciable changes. The apparent disorder which was present in the nonpolar region in the X-ray structure was removed upon minimization, resulting in fully extended aliphatic chains with carbon–carbon dihedral angles close to 180°. Thus it might be said that the minimized structure effectively corresponds to a lower temperature structure than does the X-ray structure, in that the disorder present in the latter structure was frozen out. The chain tilt angle increased by several degrees, which compensated for the lengthening of the aliphatic chains. Minimization also resulted in a rotation of the aliphatic chains in such a way as to make the carbon planes mutually coplanar. These whole chain rotations were the result of rotations about bonds mainly in the vicinity of the ester groups. The largest change was in $\gamma 1$ of DMPC2 (see Table III).

It was of interest to find out whether the large rotation in $\gamma 1$ of DMPC2 was driven by intramolecular interactions or by crystal packing considerations. A restricted energy minimization was carried out in order to see if a local energy minimum could be found in which the γ chain ester angles were close to the initial structure angles. The energy of the initial structure was minimized with respect to all variables except the bond dihedral angles in the vicinity of the ester groups of both DMPC molecules; the result of this partial minimization was then reminimized with respect to all variables, including the ester angles. This procedure did in fact locate a local minimum in which the γ chain ester angles were closer to the initial values than in structures I or II, with $\gamma 1$ being 119.6° in DMPC2. These results showed that it is indeed sterically possible to have a $\gamma 1$ angle close to 120°. The total energy of this minimized structure was 9.9 kcal/mol higher than the global minimum, however (−252.9 vs −262.8 kcal/mol, respectively); the intramolecular contribution was −60.7 kcal/mol and the intermolecular contribution was −192.2 kcal/mol. The lattice constants of this structure also differed by a greater amount from the X-ray values than did those of either structure I or II. The coordinates of this structure, which will be referred to as structure III, are in the Supplementary Material together with the coordinates of structures I and II, since it represents a distinctly different arrangement of the aliphatic chains and may perhaps occur under some conditions even though its energy is considerably higher than the global minimum as determined here.

Energy Values. Comparison of the energy components of DMPC·$2H_2O$ with the values calculated previously for lysoPE and DLPE·HAc (Vanderkooi, 1990b) shows that the interbilayer energy is considerably weaker in DMPC·$2H_2O$ than in either of these ethanolamine lipids. The average interbilayer energy per DMPC molecule (with water present) is −11.20 kcal/mol in structure I and −5.39 kcal/mol in structure II, whereas the interbilayer energies were −13.55 and −16.77 kcal/mol for lysoPE and DLPE·HAc, respectively. The intrabilayer energy of DMPC, on the other hand, is intermediate between the values previously calculated for diacyl lipids, being −3.0 kcal/mol per DMPC molecule, as compared to −3.34 and −2.55 for DLG and DLPE·HAc, respectively (Vanderkooi, 1990b).

It is of interest to compare the monolayer (lateral) energy of DMPC with that of DLPE previously calculated (Vanderkooi, 1990b). This can be done if a correction is made for the differing chain lengths. Using a value of −1.4 kcal/mol as the contribution per acyl chain CH_2 group to the lateral energy (Vanderkooi, 1990b), the anhydrous lateral energy per mole of dilauroylphosphatidylcholine is calculated as −49.6 kcal/mol, on the basis of the data given in Table VI. The monolayer energy of DLPE is considerably stronger than this, being −62.1 kcal/mol. The difference between these energies is mainly due to the intermolecular amine–phosphate hydrogen-bonding interactions between neighboring DLPE molecules in the DLPE monolayer; direct hydrogen bonding between DMPC molecules is not possible since there are no hydrogen donor groups. These computational results are consistent with the experimental observation that phosphatidylethanolamines have higher thermal phase transition temperatures than homologous phosphatidylcholines, since the low-temperature gel state is stabilized by stronger intermolecular interactions in the case of the phosphatidylethanolamines (Small, 1986).

Hydration Energy. Dry phosphatidylcholine is highly hydroscopic; Chapman et al. (1967) observed that anhydrous lecithin will pick up water even while stored over phosphorus pentoxide in a desiccator. In excess water, stacked multibilayers of dipalmitoylphosphatidylcholine in the gel state absorb sufficient water to give an equilibrium interbilayer spacing of about 20 Å (Lis et al., 1982). The equilibrium spacing is understood to be the result of a balance between long-range attractive London–van der Waals forces and a repulsive hydration force (Lis et al., 1982; Rand & Parsegian, 1984; McIntosh et al., 1987). The water content of multibilayers can be decreased by lowering the activity of the bulk water in equilibrium with the multibilayer, as for example by increasing the osmolality of the bulk water. By such means it was shown that the excess chemical potential of the interbilayer water decreases exponentially as a function of distance from the bilayer surface (Lis et al., 1982). In another study, it was estimated that it takes 2.3 kcal to reduce the number of hydrated water molecules from 23 to 2 per mole of egg lecithin (McIntosh et al., 1987); the final two water molecules were bound too tightly to be removed be the methods employed.

Other physical measurements also give evidence for the altered thermodynamic properties of water associated with phospholipids. Differential scanning calorimetry measurements by Ladbrook and Chapman (1969) indicated that 10 mol of water per mole of lecithin does not take part in the water to ice phase transition at 0 °C; they also noted that freezing of these water molecules does not occur down to −100 °C. Deuterium NMR measurements on lecithin–D_2O mixtures also showed that water associated with the lecithin is motionally restricted (Salsbury et al., 1972).

It is possible to obtain an estimate of the average binding energy of the two most tightly bound water molecules which are present in the DMPC crystal from the computational results presented here. The binding energy is calculated as the difference in energy between that of the energy-minimized hydrated crystal and the energy-minimized anhydrous crystal plus water vapor at 0 °C:

$$2\mathrm{DMPC}\cdot 4H_2O(\text{minimized}) \rightarrow 2\mathrm{DMPC}(\text{minimized}) + 4H_2O(\text{vapor})$$

Complete energy minimization was carried out on the anhydrous crystal and resulted in a value of −205.9 kcal/mol at the energy minimum. The minimum energy of the hydrated crystal is given in Table V as −262.8 kcal/mol. The intermolecular energy of the water vapor is zero and hence does not contribute to the energy of the products of the dehydration reaction. (The intramolecular energy of the water is also zero by the computational methods employed.) The energy required for the removal of the 4 mol of water is therefore 56.9 kcal, or 14.2 kcal/mol. This figure may be compared with the computed sublimation energy of ice, which is 11.66 kcal/mol. The result shows that it takes more energy to remove water from DMPC·$2H_2O$ than is does to sublime ice, which is consistent with the experimental observations mentioned above. The results indicate that conversion of the bound water to ordinary ice is an endothermic process requiring on the order of 2.5 kcal/mol.

Electrostatic forces between DMPC and water are responsible for the considerable strength of the hydration interaction. The computed electrostatic binding energy for water in DMPC is −6.4 kcal/mol, as compared to −4.3 kcal/mol in ice. The nonbonded plus hydrogen-bonded terms are similar in DMPC and in ice, being −7.8 kcal/mol in DMPC and −7.4 kcal/mol in ice. It may be concluded from these calculations that the charge–dipole interactions between water and the phosphate groups provide the basis for the strong hydration interaction.

ACKNOWLEDGMENTS

I am grateful to Dr. R. W. Pearson for supplying the X-ray coordinates of DMPC·$2H_2O$.

SUPPLEMENTARY MATERIAL AVAILABLE

One table giving the atomic coordinates for three energy-minimized DMPC·$2H_2O$ crystal structures (15 pages). Ordering information is given on any current masthead page.

Registry No. DMPC·$2H_2O$, 72884-91-4.

REFERENCES

Basti, M. M., & LaPlanche, L. A. (1990) *Chem. Phys. Lipids 54*, 99–113.

Benedict, W. S., Gailar, N., & Plyler, E. K. (1956) *J. Chem. Phys. 24*, 1139–1165.

Brasseur, R., Goormaghtigh, E., & Ruysschaert, J. M. (1981) *Biochem. Biophys. Res. Commun. 103*, 301–310.

Büldt, G., Gally, H. U., Seelig, J., & Zaccai, G. (1979) *J. Mol. Biol. 134*, 673–691.

Chapman, D., Williams, R. M., & Ladbrooke, B. D. (1967) *Chem. Phys. Lipids 1*, 444–475.

DeLoof, H., Harvey, S. C., Segrest, J. P., & Pastor, R. W. (1991) *Biochemistry 30*, 2099–2113.

Elder, M., Hitchcock, P., Mason, R., & Shipley, G. G. (1977) *Proc. R. Soc. London A 354*, 157–170.

Frischleder, H. (1978) *Chem. Phys. Lipids 22*, 343–352.

Frischleder, H. (1980) *Chem. Phys. Lipids 27*, 83–92.

Frischleder, H., & Lochmann, R. (1979) *Int. J. Quantum Chem. 16*, 203–213.

Hauser, H., Pascher, I., Pearson, R. H., & Sundell, S. (1981) *Biochim. Biophys. Acta 650*, 21–51.

Hauser, H., Pascher, I., & Sundell, S. (1988) *Biochemistry 27*, 9166–9174.

Hitchcock, P. B., Mason, R., Thomas, K. M., & Shipley, G. G. (1974) *Proc. Natl. Acad. Sci. U.S.A. 71*, 3036–3040.

Kreissler, M., Lemaire, B., & Bothorel, P. (1983) *Biochim. Biophys. Acta 735*, 12–22.

Ladbrooke, B. D., & Chapman, D. (1969) *Chem. Phys. Lipids 3*, 304–367.

Lis, L. J., McAlister, M., Fuller, N., & Rand, R. P. (1982) *Biophys. J. 37*, 657–666.

McAlister, J., Yathindra, N., & Sundaralingam, M. (1973) *Biochemistry 12*, 1189–1195.

McIntosh, T. J., Magid, A. D., & Simon, S. A. (1987) *Biochemistry 26*, 7325–7332.

Momany, F. A., Carruthers, L. M., McGuire, R. F., & Scheraga, H. A. (1974) *J. Phys. Chem. 78*, 1595–1620.

Nêmethy, G., & Scheraga, H. A. (1977) *J. Phys. Chem. 80*, 928–931.

Pascher, I., & Sundell, S. (1981a) *J. Mol. Biol. 153*, 791–806.

Pascher, I., & Sundell, S. (1981b) *J. Mol. Biol. 153*, 807–824.

Pascher, I., & Sundell, S. (1986) *Biochim. Biophys. Acta 855*, 68–78.

Pastor, R. W., Venable, R. M., & Karplus, M. (1991) *Proc. Natl. Acad. Sci. U.S.A. 88*, 892–896.

Pearson, R. H., & Pascher, I. (1979) *Nature 281*, 499–501.

Pullman, B., & Saran, A. (1975) *Int. J. Quantum Chem., Quantum Biology Symp. 2*, 71–97.

Rand, R. P., & Parsegian, V. A. (1984) *Can. J. Biochem. Cell Biol. 62*, 752–759.

Rossini, F. D., Wagman, D. D., Evans, W. H., Levine, S., & Jaffe, I. (1952) *Selected Values of Chemical Thermodynamic Properties*, NBS Circular 500, Part I, p 539.

Salsbury, N. J., Darke, A., & Chapman, D. (1982) *Chem. Phys. Lipids 8*, 142–151.

Sippl, M. J., Nêmethy, G., & Scheraga, H. A. (1984) *J. Phys. Chem. 88*, 6231–6233.

Small, D. M. (1986) *The Physical Chemistry of Lipids: From Alkanes to Phospholipids* (*Handbook of Lipid Research*) (Hanahan, D. J., Ed.) Vol. 4, pp 627–635, Plenum Press, New York.

Sundaralingam, M. (1972) *Ann. N.Y. Acad. Sci. 195*, 324–355.

Vanderkooi, G. (1973) *Chem. Phys. Lipids 11*, 148–170.

Vanderkooi, G. (1983) *J. Phys. Chem. 87*, 5121–5129.

Vanderkooi, G. (1990a) *J. Phys. Chem. 94*, 4366–4372.

Vanderkooi, G. (1990b) *Chem. Phys. Lipids 55*, 253–264.

Weiner, S. J., Kollman, P. A., Case, D. A., Chandra-Singh, U., Ghio, C., Alagona, G., Profeta, S., Jr., & Weiner, P. (1984) *J. Am. Chem. Soc. 106*, 765–784.

Wendoloski, J. J., Kimatian, S. J., Schutt, C. E., & Salemme, F. R. (1989) *Science 243*, 636–638.

Whalley, E. (1957) *Trans. Faraday Soc. 53*, 1578–1585.

Wyckoff, R. W. G. (1963) *Crystal Structures* 2nd ed., Vol. 1, pp 322–324, Wiley, New York.

Zaccai, G., Büldt, G., Seelig, A., & Seelig, J. (1979) *J. Mol. Biol. 134*, 693–706.